JOURNAL OF PROPULSION AND POWER
Vol. 10, No. 2, March–April 1994

Inlet Velocity Profile Effects on Turbulent Swirling Flow Predictions

Mingchun Dong* and David G. Lilley†
Oklahoma State University, Stillwater, Oklahoma 74078

The validity of flowfield predictions resulting from the choice of inlet velocity profiles is assessed. Results demonstrate that realistic predictions are forthcoming only from the inclusion of realistic axial, radial, and swirl velocity profile as inlet conditions. The ensuing flowfields are characterized by means of velocity profile and streamline patterns, and illustrate the large-scale effects of inlet swirl and velocity profiles on flowfields. Clearly, measured inlet profiles must be used in future turbulence modeling development studies for improved simulation of flowfields.

I. Introduction

DESIGNERS of gas turbine combustors are aided by lengthy and costly experimentation on full-scale hardware. These experiments can be diminished in number and economical design practices greatly facilitated by the availability and understanding of prior predictions of the combustor flowfield obtained by the use of mathematical models incorporating numerical prediction procedures. Such work combines the rapidly developed fields of theoretical combustion aerodynamics and computational fluid dynamics, and their continued improvement and use will significantly reduce the time and cost of combustor development programs.[1,2] Consequently, a phenomenological modeling approach to combustor design, supplemented by key experiments which depict the fundamental physical phenomena present within combustors, now is feasible and a necessity in minimizing combustor development time and cost requirements.

This article is concerned with the two-dimensional axisymmetric modeling approach with emphasis placed on various inlet velocity profile effects on the nonreacting flowfield (velocities and turbulence levels). The well-known k-e turbulence model is used. It is conceded that more advanced models might be more accurate, but even this relatively simple model illustrates the dramatic effects of inlet profiles on the predictions, the main emphasis of our study. When a verified more advanced model is available, it may be included. However, the present model serves to illustrate the main points of the study. Since the governing differential equations of swirling recirculating flows are elliptic and solutions depend strongly on the boundary conditions applied around the flow domain, it is important to define adequately the boundary conditions, especially the inlet velocity profiles. Yet most of the previous studies make gross simplifications regarding inlet conditions, and especially with regard to the inlet radial velocity which is often taken to be zero. Axial and swirl velocity profiles, if not measured, are often assumed to be simple flat profiles, or sometimes a flat axial profile with a solid body rotation swirl profile.

Received Nov. 12, 1992; presented as Paper 93-0133 at the AIAA 31st Aerospace Sciences Meeting, Reno, NV, Jan. 11–14, 1993; revision received June 2, 1993; accepted for publication June 28, 1993.

*Graduate Student, School of Mechanical and Aerospace Engineering. Member AIAA.
†Professor, School of Mechanical and Aerospace Engineering. Fellow AIAA.

Numerical predictions of turbulent swirling recirculating confined flows are presented using various inlet velocity starting conditions for the cases of swirl vane angles equal to 45 and 70 deg. The validity of flowfield predictions resulting from the choice of inlet profiles is assessed. Results demonstrate that realistic predictions are forthcoming only from the inclusion of realistic axial, radial, and swirl velocity profiles as inlet conditions, and that considerable errors occur if unrealistic idealized inlet conditions are used. The ensuing flowfields are characterized by means of radial profiles of axial and swirl velocities and streamline patterns, and illustrate the large-scale effects of inlet velocity profiles and swirl on flowfields.

II. Theoretical Approach

A. Idealized Velocity Profiles

All theoretical analyses of swirler performance and most numerical simulations of combustor flowfields have used simple idealized swirler exit velocity profiles. Common assumptions made include flat axial and swirl velocity profiles downstream of the swirler for swirlers with vanes of constant angle,[3–8] and a flat axial profile with a linear swirl profile (solid-body rotation) for swirlers with helicoidal vanes for tangential-entry swirl generators.[9,10] These, however, have been shown to be quite unrealistic[4,8,11] and lead to considerable errors in computer predictions of the flowfield.[12] Although the best remedy for numerical simulations is to use experimentally measured swirler exit profiles if they are available, idealized profiles are very useful in theoretical work. If more realistic profile assumptions can be developed which are still mathematically tractable, more useful analytical results may be derived. Better idealized profiles would also be useful as inlet boundary conditions for computer modeling when measured data are not available.

Measurements have shown[4] that linear and parabolic profiles of axial velocity are more appropriate for moderate and high swirl cases, and that the swirl velocity also approaches a parabolic profile at high swirl strengths, with most of the flow leaving near the outer boundary of the swirler. Several combinations of linear and parabolic idealized profiles are shown in Fig. 1, along with the flat, linear, and parabolic profile assumptions stated in the form of profile expressions. Parameters, swirl numbers, and discussions associated with these profiles are investigated in Ref. 4. Abujelala and Lilley[12] illustrated that different flowfields ensued from a different choice of inlet velocity profiles, and the degree of nozzle confinement at the exit from the flow domain. Later, empirical extensions were suggested for the k-e turbulence model, and their limitations evaluated for weakly and strongly swirling confined flows.[13] Sturgess[14] made similar observations about the effect of inlet boundary conditions, including turbulence

level and length scale at the inlet. His predictions were susceptible to the choice, and results compared unfavorably with the experimental data of Ref. 3. Sturgess et al.[15] gave predictions of several sample cases to illustrate the importance of inlet boundary conditions in prediction studies.

B. Types of Inlet Boundary Conditions Considered

Seven possible specifications of the inlet velocities are considered and the idealized axial and swirl velocity profile cases 1–5 are shown in Fig. 1. In each case the magnitudes of u_{m0}, w_{m0}, etc. (identified below) are chosen to conform to the same swirl number consistent with the appropriate swirl vane angle. In practical systems, different types of swirl-generating methods are used, e.g., tangential-entry, flat and/or curved blades with/without constant turn angle (i.e., twist). These alternate methods produce differing profiles, which are typified by the cases now considered. The equations given in Ref. 4 are used for this.

Case 1: Flat inlet axial and swirl velocities with radial velocity zero are assumed. That is, both u and w are constant valued

$$u_0 = \text{const}$$

$$w_0 = u_0 \tan \phi$$

where ϕ is the swirl vane angle.

Case 2: The same as case 1, except that the inlet swirl velocity profile is assumed to be that of solid body rotation

$$u_0 = \text{const}$$

$$w_0 = w_{m0} r/R$$

where w_{m0} is the maximum orifice value of w which occurs at the outer edge $r = R$ of the inlet. The value of w_{m0} is chosen to maintain the swirl number the same as in case 1.

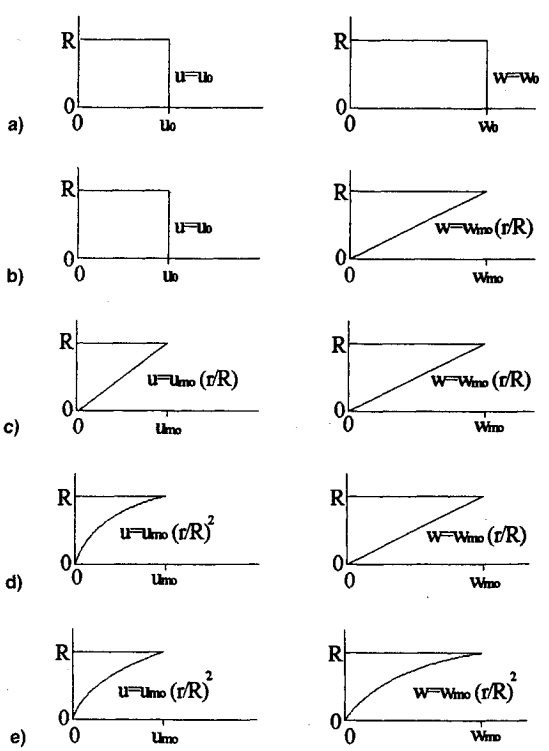

Fig. 1 Idealized axial and swirl velocity profile cases: a) case 1—flat axial and swirl profiles, b) case 2—flat axial and linear swirl profiles, c) case 3—linear axial and swirl profiles, d) case 4—parabolic axial and linear swirl profiles, and e) case 5—parabolic axial and swirl profiles.

Case 3: Linear axial and swirl velocities with radial velocity zero are assumed. That is

$$u_0 = u_{m0} r/R$$

$$w_0 = w_{m0} r/R$$

where u_{m0} is the maximum orifice value of u which occurs at the outer edge $r = R$ of the inlet. The values of u_{m0} and w_{m0} are chosen to maintain the swirl number the same as in case 1.

Case 4: Parabolic axial and linear swirl profiles with radial velocity zero are assumed. That is

$$u_0 = u_{m0}(r/R)^2$$

$$w_0 = w_{m0} r/R$$

where the values of u_{m0} and w_{m0}, as those in case 3, are chosen to maintain the swirl number the same as in case 1.

Case 5: Parabolic axial and swirl profiles with radial velocity zero are assumed. That is

$$u_0 = u_{m0}(r/R)^2$$

$$w_0 = w_{m0}(r/R)^2$$

where the values of u_{m0} and w_{m0}, as those in case 4, are chosen to maintain the swirl number the same as in case 1.

Case 6: Measured inlet axial and swirl velocities are used[4] with radial velocity assumed to be zero.

Case 7: Measured inlet axial, radial, and swirl velocity values are used.[4]

In all cases considered, inlet kinetic energy of turbulence k and its dissipation rate e are specified as in generally accepted ways.[16,17] First, the kinetic energy k is specified as a function of radial location by means of a constant multiplied by local mean axial velocity squared. The constant is taken as 0.03, which is consistent with isotropic turbulence intensity of 14% as recommended in Ref. 4. The turbulence length scale L is taken as 3% of the radius of the flow passage as recommended in Refs. 4 and 15. Then e is deduced locally from k and L. An indication of the effect of these choices on the results is given in Sec. III.A.

C. Prediction Procedure

The simulation and solution techniques focus attention directly on the primitive pressure and velocity variables. The approach is based on the semi-implicit method for pressure linked equations (SIMPLE) method.[16] The basic features of SIMPLE are as follows:

1) A finite difference procedure is used in which the dependent variables are the velocity components and pressure.

2) The pressure is deduced from an equation which is obtained by the combinations of the continuity equation and the momentum equations.

3) The idea is present at each iteration of a first approximation to the solution followed by succeeding corrections.

4) The procedure incorporates displaced grids for the axial and radial velocities u and v, which are placed between the nodes where pressure P and other variables are stored.

5) An implicit line-by-line relaxation technique is employed in the solution procedure, using the tridiagonal matrix algorithm TDMA.

The method is applied to the case of a sudden expansion from a round pipe (diameter $d = 0.15$ m) into another round pipe (diameter D) with expansion ratio $D/d = 2$. The domain length is four times that of the larger pipe diameter (D). The solution domain is covered with a nonuniform 21 × 22 grid, gradually expanding in the x direction (with expansion ratio 1.05). Iteration monitoring and final convergence is decided by way of a residual-source criterion, which measures the departure from exactness (summed over all points) for each of the variables being solved. Iteration continues until all the equations are sufficiently well-satisfied and values have stabilized throughout the flow domain. Generally, this takes

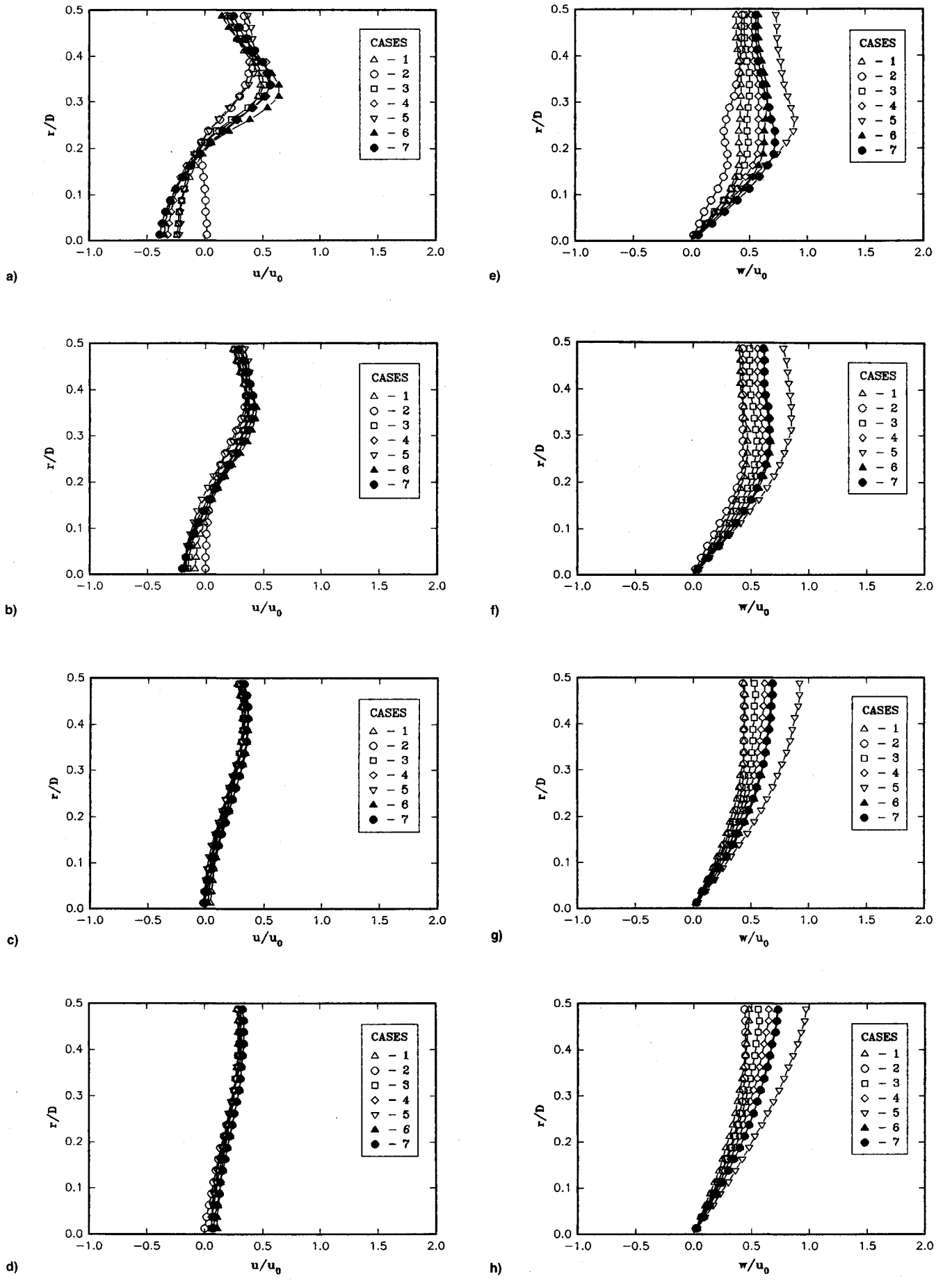

Fig. 2 Predicted velocity profiles for $\phi = 45$ deg using various inlet conditions: a) u/u_0 at $x/D = 0.5$, b) u/u_0 at $x/D = 1.0$, c) u/u_0 at $x/D = 1.5$, d) u/u_0 at $x/D = 2.0$, e) w/u_0 at $x/D = 0.5$, f) w/u_0 at $x/D = 1.0$, g) w/u_0 at $x/D = 1.5$, and h) w/u_0 at $x/D = 2.0$.

approximately 300–400 iterations, depending on the boundary conditions.

III. Flowfield Computations

Predictions are discussed which deal with the flow through the inlet swirler with vane angles set to $\phi = 45$ and 70 deg. Various types of inlet profile assumptions, cases 1–7 of Sec. II.B. are considered, and the similarity and differences in the ensuing flowfield predictions are noted.

A. Effects of Inlet Turbulence Quantities on Predicted Results

Taking measured inlet velocity components u, v, and w (case 7) with L specified as 3% of the characteristic dimension (radius) of the flow passage, predictions were made for swirl vane angle $\phi = 45$ and 70 deg with turbulence intensities of 8, 14, and 26%, respectively. Over this range of variance of turbulence intensity, predicted axial and swirl velocity profiles did not change much further downstream. However, the (small) magnitude of negative axial velocity in the central recirculation zone approximately doubled. Other predictions were made with turbulence intensity held at 14%, while the length scale varied over the range 1, 3, and 10% of the radius of the flow passage. Over this range of variance of length scale, profiles of axial and swirl velocities did not change much. Again, the most dramatic effect was seen in the magnitude of the negative axial velocity in the central recirculation zone, which approximately halved. In the following analysis, the turbulence intensity is specified as 14%, and L as 3% of the characteristic dimension of the flow passage, as recommended in Refs. 4 and 15.

B. Effects of Inlet Velocity Profiles

1. Swirl Vane Angle $\phi = 45$ Deg

Consider first the flowfield resulting when the inlet swirl vane angle is 45 deg. Figure 2 shows predicted axial and swirl velocity profiles at various downstream axial stations, $x/D = 0.5, 1.0, 1.5$, and 2.0, obtained when the inlet velocity profiles are specified by the following:

Case 1: Flat u and w profiles, with v zero
Case 2: Flat u profile, with solid body rotation w, and v zero
Case 3: Linear u and w profiles, with v zero
Case 4: Parabolic u and linear w, with v zero
Case 5: Parabolic u and w, with v zero
Case 6: Measured u and w, with v zero
Case 7: Measured u, v, and w

These are discussed in greater detail in Sec. II.B. The flowfield structure for these seven cases is further illustrated by way of streamline shady plots which are computer calculated and drawn in Fig. 3. The figure is stretched in the radial direction by 50% to aid observation. This same streamline stretch is retained in all subsequent streamline plots. Inspection of these figures is quite revealing and may be assessed in the light of pitot probe experimental data.[3] Figure 4 shows the starting and terminating locations of the central toroidal recirculation zones (CTRZ) for seven different test cases and the corresponding experimental measurements. The starting and terminating locations of the CTRZ are specified as s and $(s + l)$, respectively, where s is the distance from inlet and l is the length of the CTRZ. The blockage ratio, W/D, or the width W of the CTRZ is shown in Fig. 5 for seven different test cases and the corresponding measurements.[3]

Cases 3–7 covered in Figs. 2–5 give central recirculation zones terminating at about $x/D = 1.5$, with a central recirculation zone similar to that found in practice in length and width. But initial spreading rates vary considerably: only in cases 6 and 7 does the central recirculation zone begin immediately on entry to the large chamber, with case 7 spreading most rapidly in the initial region. Cases 1 and 2 do not possess enough centrifugal effect because of their unrealistic inlet swirl velocity profiles, resulting in predictions of short and narrow central recirculation zones. Also, cases 1–6 do not have a radial component of velocity to encourage inlet radial spreading of the streamlines. These inlet flow ideas may be confirmed by observing the size of the corner recirculation zone. Cases 2, 5, and 7 exhibit shorter corner zones, with only case 7 also possessing the correct central activity near the inlet—rapid spreading with a central recirculation flow

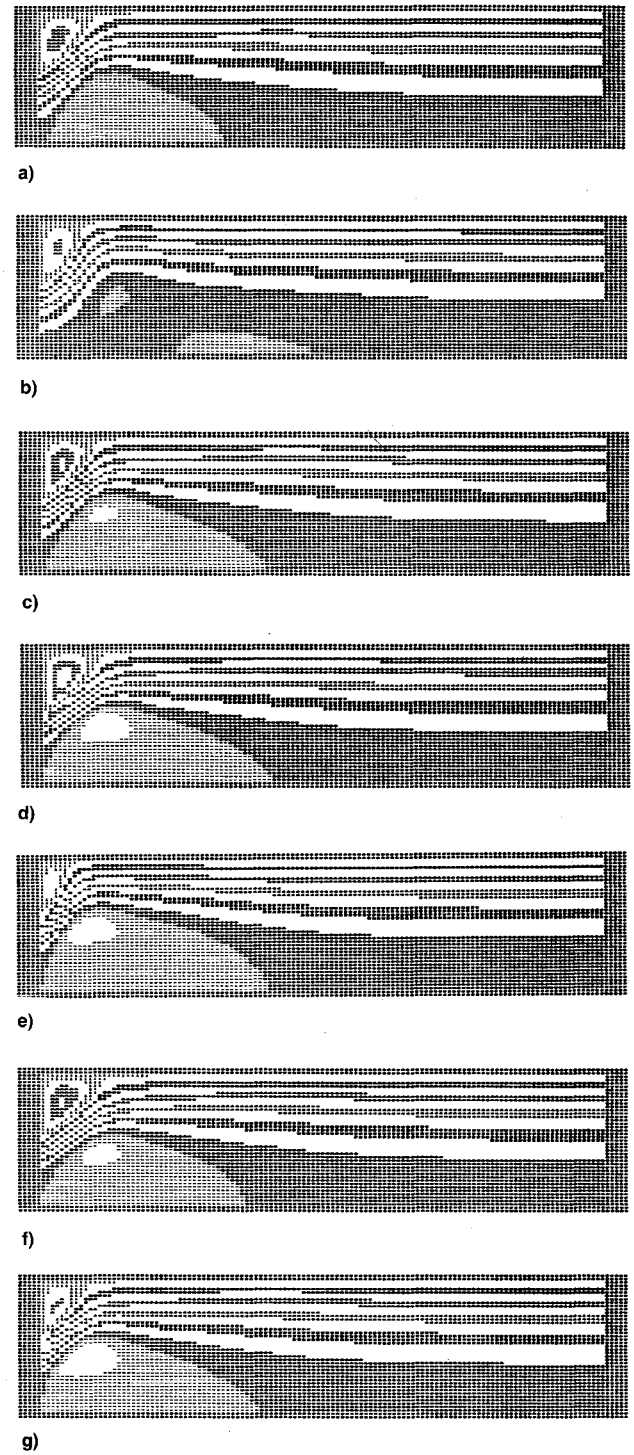

Fig. 3 Predicted streamlines for $\phi = 45$-deg flowfield using various inlet conditions: a) case 1—flat axial and swirl profiles, b) case 2—flat axial and linear swirl profiles, c) case 3—linear axial and swirl profiles, d) case 4—parabolic axial and linear swirl profiles, e) case 5—parabolic axial and swirl profiles, f) case 6—measured inlet axial and swirl velocities, and g) case 7—measured inlet axial, radial, and swirl velocities.

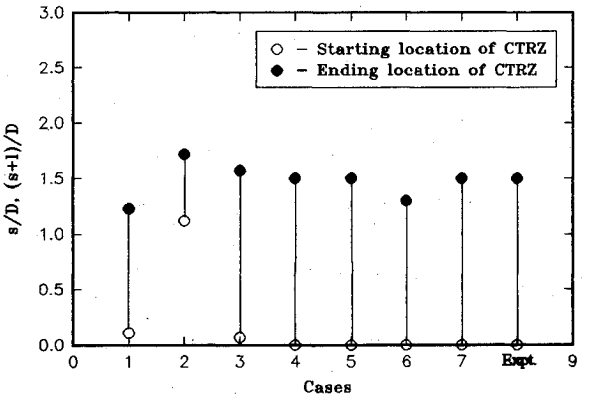

Fig. 4 Location of central recirculation zone on x axis for swirl vane angle = 45 deg.

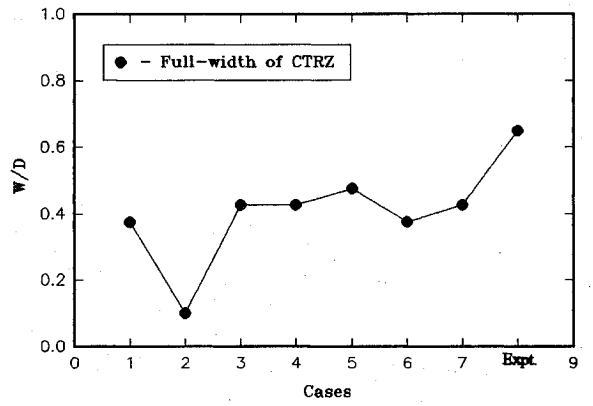

Fig. 5 Full width of central recirculation zone for swirl vane angle = 45 deg.

beginning immediately. None of the predictions match the precessing vortex core details found in flow visualization studies[18] or the negative axial velocities measured by pitot probe experimentation[3] near the facility axis $r/D < 0.1$, extending all the way to the test section exit. Nevertheless, comparison of the predictions with the gross features of the corresponding experimental data[3] clearly indicates that the inlet conditions of case 7 are superior in allowing realistic flowfield prediction.

2. Swirl Vane Angle ϕ = 70 Deg

Figure 6 corresponds to Fig. 3, Figs. 7 and 8 correspond to Figs. 4 and 5, but with the swirl vane angle increased to 70 deg. A figure of predicted axial and swirl velocity profiles with inlet swirl vane angle equal to 70 deg is available in Ref. 19. The trends parallel those observed with vane angle equal to 45 deg, shown in Fig. 2. Now the strong centrifugal forces present in the incoming flow play their part. Initial spreading rates are very high with very small corner recirculation zones in all cases, except that of cases 6 and 7 seen in Fig. 6. All central recirculation zones, except case 2, begin immediately at the inlet and are much wider and longer than those with ϕ = 45 deg. Those of cases 1–5 are initially very wide and long, much wider and longer than the measurements[3] indicate (Figs. 6–8). This results from unrealistically large centrifugal forces attributable to unrealistically large swirl velocity magnitudes. With zero inlet radial velocity, case 6 does not spread rapidly enough at the inlet and a long central recirculation zone extending to x/D = 1.9 is predicted. With the inclusion of the correct inlet radial velocity, a recirculation zone much more like that found experimentally results in case 7.

C. Effects of Swirl

Predicted streamline patterns for swirl vane angles of 45 and 70 deg for cases 1–7 are shown in Figs. 3 and 6, parts

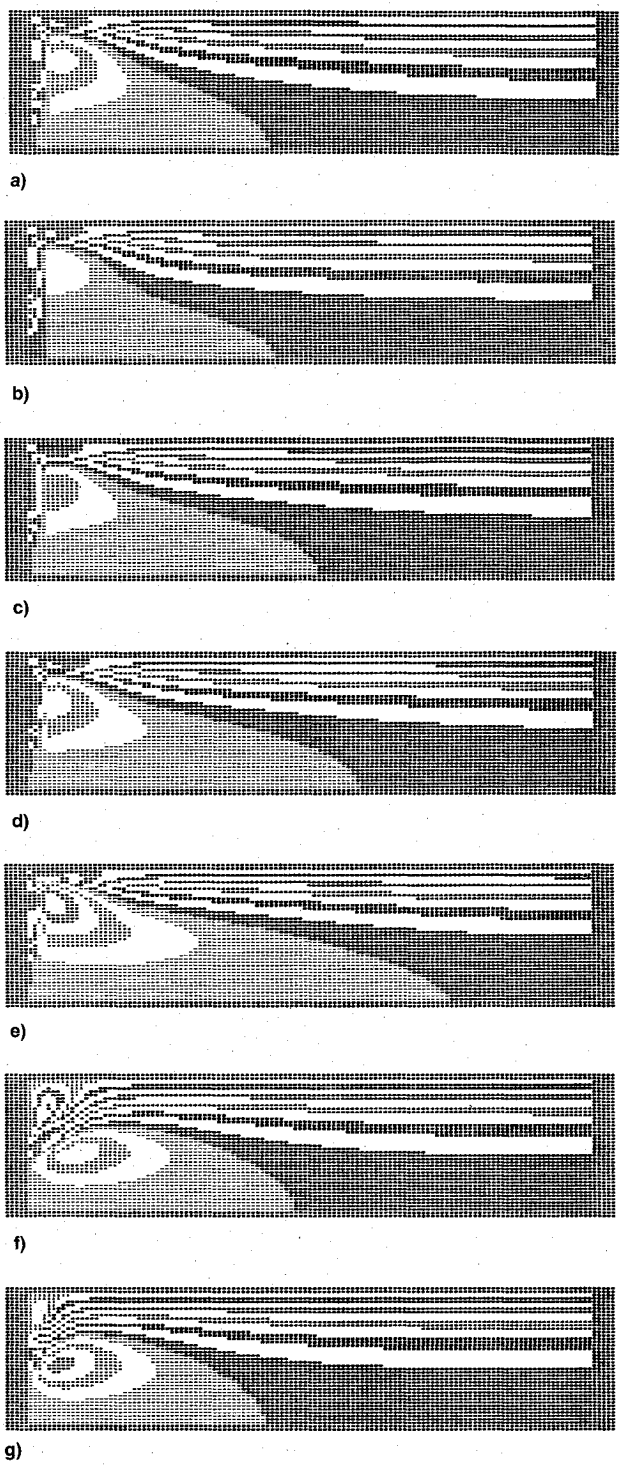

Fig. 6 Predicted streamlines for ϕ = 70-deg flowfield using various inlet conditions: a) case 1—flat axial and swirl profiles, b) case 2—flat axial and linear swirl profiles, c) case 3—linear axial and swirl profiles, d) case 4—parabolic axial and linear swirl profiles, e) case 5—parabolic axial and swirl profiles, f) case 6—measured inlet axial and swirl velocities, and g) case 7—measured inlet axial, radial, and swirl velocities.

a–g, respectively. The predicted effects of swirl shown in these figures confirm in general the well-known ideas about swirl effects on axisymmetric turbulent confined jet flows. Under nonswirling conditions, a large corner recirculation zone exists and the centerline axial velocity changes gradually from its inlet value as downstream development occurs. However, as the degree of inlet swirl is 45 deg, axial velocity profiles change dramatically. Near the inlet a central toroidal recirculation zone appears and the corner recirculation zone

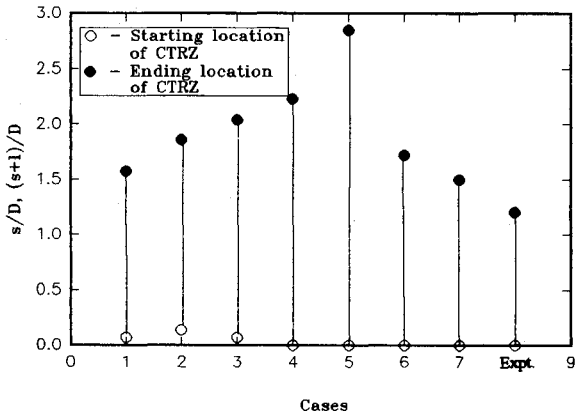

Fig. 7 Location of central recirculation zone on x axis for swirl vane angle = 70 deg.

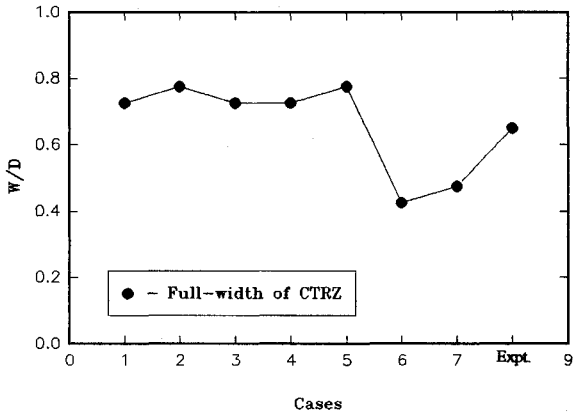

Fig. 8 Full width of central recirculation zone for swirl vane angle = 70 deg.

shortens considerably. Under strong swirl conditions of ϕ equal to 70 deg, a much wider central recirculation region is established. It promotes a very large forward velocity near the confining walls rather than a corner recirculation region.

These predicted effects generally agree with the experimental data, except that precessing vortex core regions of solid body rotation back flow, which occur downstream of central recirculation regions in the swirl flow cases investigated,[2] are not well predicted. Only the 70-deg case predicts almost zero axial velocity on the centerline extending to $x/D = 4$. The central recirculation zone is predicted to be longer than found in practice. Also, swirl velocity profiles do not match well the experimental data—the radial location of swirl velocity maximum value occurs too close to the confining chamber walls rather than occurring abruptly at the edge of a vortex core region. The observed discrepancies may be because of poor probe sensitivity in turbulent low velocity regions, and/or poor turbulence model performance in these regions. Only further detailed hot-wire and/or laser Doppler anemometer measurements and turbulence model development will resolve the inconsistencies. Clearly, measured inlet profiles must be used in future turbulence modeling development studies for improved simulation of this flowfield.

IV. Closure

A numerical prediction using the standard two-equation k-e turbulence model and different inlet flow boundary condition assumptions has been applied to a confined swirling flow. Inlet flow boundary conditions have been demonstrated to be extremely important in simulating a flowfield by means of numerical calculations. Predictions with flat, linear, or parabolic inlet axial and swirl velocity profiles, or a combination of these profiles with zero radial velocity, are shown to be inappropriate. Realistic predictions are forthcoming only from the inclusions of realistic axial, radial, and swirl velocity profile as inlet conditions. Clearly, measured inlet profiles must be used in future turbulence modeling development studies for improved simulation of flowfields.

References

[1]Gupta, A. K., and Lilley, D. G., "Flowfield Modeling and Diagnostics," Abacus Press, Tunbridge Wells, England, UK, 1985.

[2]Gupta, A. K., Lilley, D. G., and Syred, N., "Swirl Flows," Abacus Press, Tunbridge Wells, England, UK, 1984.

[3]Yoon, H. K., and Lilley, D. G., "Five-Hole Pitot Probe Time-Mean Velocity Measurements in Confined Swirling Flows," AIAA Paper 83-0315, Jan. 1983.

[4]Sander, G. F., and Lilley, D. G., "The Performance of an Annular Vane Swirler," AIAA Paper 83-1326, June 1983.

[5]Rhode, D. L., Lilley, D. G., and McLaughlin, D. K., "On the Prediction of Swirling Flowfields Found in Axisymmetric Combustor Geometries," *Journal of Fluids Engineering*, Vol. 104, Sept. 1982, pp. 378–384.

[6]Rhode, D. L., Lilley, D. G., and McLaughlin, D. K., "Mean Flowfields in Axisymmetric Combustor Geometries with Swirl," *AIAA Journal*, Vol. 21, No. 4, 1983, pp. 593–600.

[7]Kerr, N. M., and Fraser, D., "Swirl. Part I: Effect on Axisymmetrical Turbulent Jets," *Journal of the Institution of Fuel*, Vol. 38, Dec. 1965, pp. 519–526.

[8]Mathur, M. L., and MacCallum, N. R. L., "Swirling Air Jets Issuing from Vane Swirlers. Part I: Free Jets; Part II: Enclosed Jets," *Journal of the Institution of Fuel*, Vol. 40, May 1967, pp. 214–245.

[9]Chigier, N. A., and Chervinsky, A., "Experimental Investigation of Swirling Vortex Motion in Jets," *Journal of Applied Mechanics*, Vol. 34, June 1967, pp. 443–451.

[10]Beer, J. M., and Chigier, N. A., "Combustion Aerodynamics," Applied Science Publishers, London, 1972.

[11]Beltagui, S. A., and MacCallum, N. R. L., "Aerodynamics of Vane-Swirled Flames in Furnaces," *Journal of the Institution of Fuel*, Vol. 49, Dec. 1976, pp. 183–193.

[12]Abujelala, M. T., and Lilley, D. G., "Confined Swirling Flow Predictions," AIAA Paper 83-0316, Jan. 1983.

[13]Abujelala, M. T., and Lilley, D. G., "Limitations and Empirical Extensions of the k-e Model as Applied to Turbulent Confined Swirling Flows," AIAA Paper 84-0441, Jan. 1984.

[14]Sturgess, G. J., "Aerothermal Modeling Phase I," Pratt & Whitney Aircraft, NASA CR-168202, East Hartford, CT, May 1983.

[15]Sturgess, G. J., Syed, S. A., and McManus, K. R., "Importance of Inlet Boundary Conditions for Numerical Simulation of Combustor Flows," AIAA Paper 83-1263, June 1983.

[16]Lilley, D. G., and Rhode, D. L., "A Computer Code for Swirling Turbulent Axisymmetric Recirculating Flows in Practical Isothermal Combustor Geometries," NASA CR-3442, Feb. 1982.

[17]Launder, B. E., and Spalding, D. B., "The Numerical Computation of Turbulent Flows," *Computational Methods in Applied Mechanics and Engineering*, Vol. 3, March 1974, pp. 269–289.

[18]Lilley, D. G., "Swirling Flows in Typical Combustor Geometries," *Journal of Propulsion and Power*, Vol. 2, No. 1, 1986, pp. 64–72.

[19]Dong, M., and Lilley, D. G., "Inlet Velocity Profile Effects on Turbulent Swirling Flow Predictions," AIAA Paper 93-0133, Jan. 1993.